Structures and Stabilities of Endo- and Exohedral Dodecahedrane Complexes ($X@C_{20}H_{20}$ and $XC_{20}H_{20}$, $X = H^+$, H, N, P, C^-, Si^-, O^+, S^+)

Zhongfang Chen,[†,‡] Haijun Jiao,[§,||] Damian Moran,[†,‡] Andreas Hirsch,*[,†] Walter Thiel,[⊥] and Paul von Ragué Schleyer*[,†,‡]

Institut für Organische Chemie, Universität Erlangen-Nürnberg, Henkestrasse 42, 91054 Erlangen, Germany, Computational Chemistry Annex, University of Georgia, Athens, Georgia 30602-2525, Department of Chemistry, Shanxi Normal University, 041004 Linfen, P. R. China, Leibniz-Institut für Organische Katalyse an der Universität Rostock e.V., Buchbinderstrasse 5-6, 18055 Rostock, Germany, and Max-Planck-Institut für Kohlenforschung, 45466 Mülheim an der Ruhr, Germany

Received: October 31, 2002; In Final Form: January 23, 2003

B3LYP/6-31G* computations predict the relative energies and stabilities of the endohedral ($X@C_{20}H_{20}$) and exohedral ($XC_{20}H_{20}$) dodecahedrane complexes ($X = H^+$, H, N, P, C^-, Si^-, O^+, S^+). H^+ does not bind endohedrally but bridges a C−C bond exohedrally; the proton affinity is 185.3 kcal/mol. Except for O^+, all other guest species (H, N, P, C^-, Si^-, S^+) are minima at the cage center. The H-atom inclusion energy is similar to that of helium (36.3 vs 38.0 kcal/mol), whereas the other endohedral complexes have much higher inclusion energies (125−305 kcal/mol). In all cases, the endohedral complexes are energetically less favorable than their exohedral isomers. $C_{20}H_{21}$ has a cage-ruptured structure, whereas N, P, and their isoelectronic analogues have exohedral structures and bind as doublet states to broken cage C−C bonds. Endohedral H, N, C^-, O^+, and S^+ preserve their unencapsulated ground states, whereas P and Si^- interact strongly with the cage and lose their atomic ground-state character.

Introduction

Dodecahedrane (**1**, $C_{20}H_{20}$),[1] a fascinating molecule with unusually high symmetry (I_h), has been studied at various levels of theory with regard to the energy,[2,3] vibrational frequencies,[4] inelastic neutron-scattering spectrum,[5] substituent effects,[6] and charge density.[7] The synthesis of **1**, a difficult challenge, was first achieved by Paquette[8] and later by Prinzbach[9] using improved routes. The availability of **1** enabled chemical and physical studies on its thermochemistry, strain energy,[10] and C−H bond dissociation energy.[11] Dodecahedranes' "outside chemistry" has been investigated intensively,[12] with its high-voltage dehydrogenation into C_{20},[13] the smallest fullerene, the most dramatic experiment reported to date. The "inside chemistry" of **1** exploits its cage structure, and the possible encapsulation of various guest atoms and ions has been investigated.[3a,b,14,15] A helium atom has been "shot" into **1** to obtain stable $He@C_{20}H_{20}$[16] by using an experimental procedure developed for fullerenes.[17] This encapsulated species is fascinating because the steric compression within the cavity is severe and the barrier to penetrating intact **1** must be very high. Following earlier theoretical investigations, Schleyer et al.[15c] recently computed the structures and stabilities of 14 different endohedral dodecahedrane complexes ($X@C_{20}H_{20}$, X = H, He, Ne, Ar, $Li^{0/+}$, $Be^{0/+/2+}$, $Na^{0/+}$, $Mg^{0/+/2+}$). Helium encapsulation (37.9 kcal/mol) was ∼2 kcal/mol less favorable than hydrogen encapsulation (35.8 kcal/mol) but >12 kcal/mol better than the next most stable endohedral dodecahedrane complex, $Li@C_{20}H_{20}$ (50.6 kcal/mol).

Recently, endohedral fullerenes whose dopant atoms retain their isolated atomic states received attention, partly because of newly proposed solid-state quantum computers based on such materials.[18] Experimentally, C_{60}-encapsulated tritium,[19] nitrogen,[20] and phosphorus[21] have already been successfully prepared. Similarly, atomic hydrogen encapsulated in fully deuterated **1** ($C_{20}D_{20}$) also has been proposed for use as single quantum bits (quabits) in solid-state quantum computers.[18d] Theoretical calculations have predicted that it may be possible to implant H atoms within the surface layer of fullerene molecules.[22]

The previous investigations into endohedral complexes of **1** have left many questions unanswered. As a cage hydrocarbon, to what extent does **1** bind a proton? Can neutral atoms such as H, N, P, and their isoelectronic charged analogues (C^-, Si^-, O^+, S^+) also reside at the center of **1**? What are their electronic states when encapsulated in **1**? Is it possible to use these endohedrally doped dodecahedrane complexes as solid-state quantum bits? This paper addresses these questions by computing the structures and stabilities of endohedral $X@C_{20}H_{20}$ ($X = H^+$, H, N, P, C^-, S^-, O^+, S^+) complexes and their exohedral isomers.

Computational Details

All calculations were carried out at the (U)B3LYP/6-31G* density functional level of theory using Gaussian 98.[23] Guest atoms or ions were placed at the cage centers (I_h) of endohedral

* Corresponding authors. A.H. E-mail: andreas.hirsch@organik.uni-erlangen.de; Fax.: +49 9131 85 26864. P.v.R.S. E-mail: schleyer@chem.uga.edu.
† Universität Erlangen-Nürnberg.
‡ University of Georgia.
§ Shanxi Normal University.
|| Universität Rostock e.V.
⊥ Max-Planck-Institut für Kohlenforschung.

10.1021/jp0273631 CCC: $25.00
Published on Web 03/01/2003

TABLE 1: B3LYP/6-31G* Optimized Endohedral Complex (I_h) Absolute Energies (au), Zero-Point Energies (ZPE; kcal/mol, unscaled), Lowest Vibrational Frequencies (ω_1; cm^{-1}) (or Imaginary Frequencies) and Optimized Bond Lengths (Å)

	energy	ZPE	ω_1	R_{C-X}	R_{C-C}	R_{C-H}
$C_{20}H_{20}$	−774.18503	225.59	479.1	2.181	1.557	1.095
$H^+@C_{20}H_{20}$	−774.29342	213.82	−1251.6i(12)[a]	2.191	1.564	1.093
$^2H@C_{20}H_{20}$	−774.63243	228.77	490.4	2.189	1.562	1.096
$^4N@C_{20}H_{20}$	−828.56724	223.89	480.2	2.218	1.583	1.097
$^4P@C_{20}H_{20}$	−1114.94712	214.40	349.3	2.253	1.608	1.105
$^4C^-@C_{20}H_{20}$	−811.83448	219.15	511.7	2.211	1.578	1.110
$^4Si^-@C_{20}H_{20}$	−1063.07519	206.44	313.6	2.238	1.597	1.122
$^4O^+@C_{20}H_{20}$	−848.75284	217.80	−282.7i(3)[a]	2.216	1.582	1.094
$^4S^+@C_{20}H_{20}$	−1171.60325	218.32	347.6	2.261	1.614	1.095

[a] Higher-order saddle point, with the number of imaginary frequencies given in parentheses.

TABLE 2: B3LYP/6-31G* Endohedral Complex Inclusion Energies (E_{inc}; kcal/mol), Natural Charges (q), and Spin Densities (S)

	E_{inc}	q_X	q_C	q_H	S_X	S_{Cn}[a]	S_H
empty $C_{20}H_{20}$			−0.25	0.25			
$H^+@C_{20}H_{20}$	−79.6	0.79	−0.29	0.30			
$^2H@C_{20}H_{20}$	36.3	0.08	−0.25	0.25	0.91	0.00	0.01
$^4N@C_{20}H_{20}$	125.3	−0.05	−0.25	0.25	2.57	0.00	0.02
$^4P@C_{20}H_{20}$	300.3	1.07	−0.29	0.24	1.73	0.01	0.06
$^4C^-@C_{20}H_{20}$	115.9	−0.36	−0.24	0.21	2.12	0.00	0.05
$^4Si^-@C_{20}H_{20}$	305.2	1.52	−0.31	0.19	0.93	0.02	0.09
$^4O^+@C_{20}H_{20}$	−21.0	0.46	−0.26	0.29	2.23	0.02	0.02
$^4S^+@C_{20}H_{20}$	182.22	0.88	−0.28	0.29	2.06	0.01	0.03

[a] The spin density of the carbon neighboring X (as shown in Figure 2).

complexes, and skeletally bonded C_{2v} and C_s symmetries were used for their exohedral isomers. Optimized structures were characterized by frequency calculations as energy minima (zero imaginary frequencies; $N_{imag} = 0$) or saddle points (≥ 1 imaginary frequency; $N_{imag} \geq 1$). Mode following and optimization were used to locate the corresponding minima when imaginary frequencies were encountered. Zero-point energies (ZPE), derived from the vibrational frequency analysis of equilibrium geometries, were scaled by 0.9804. Atomic charges were evaluated using natural bond orbital (NBO) analysis.[24]

The inclusion energies (E_{inc}) of endohedral complexes were evaluated by comparing the energy of $X@C_{20}H_{20}$ with the sum of the energies of the isolated components, $C_{20}H_{20}$ and X. For comparison, the corresponding exohedral binding energies (E_{bind}) also were computed. The ZPE-corrected energy difference between the most stable exohedral structures and their endohedral isomers was defined as the isomerization energy (E_{isom}). Optimized bond lengths and lowest real (or imaginary) frequencies for I_h dodecahedrane and $X@C_{20}H_{20}$ derivatives are summarized in Table 1, and their inclusion energies (E_{inc}) as well as the natural charge (q) and spin densities (S) are shown in Table 2. The optimized geometries of exohedral complexes are given in Figure 3 and Table 3, and their exohedral binding energies (E_{bind}) and endo−exo isomerization energies (E_{isom}) are summarized in Table 4.

Results and Discussion

$H^+@C_{20}H_{20}$. Is an endohedral proton complex possible? To alleviate its extreme electron deficiency, H^+ tends to attach itself to lone pairs or to bonds. Disch and Schulman[14a] postulated that the exterior of **1** might be protonated more favorably than the interior. Indeed, I_h geometry-optimized $H^+@C_{20}H_{20}$ has $N_{imag} = 12$ and represents a high-order saddle point. Mode following reveals that the proton migrates out of the cage without barrier during optimization. This results in an exterior-protonated isomer (C_{2v}, Figure 1a), $C_{20}H_{21}^+$, in which the proton bridges two carbon atoms symmetrically and separates them by 2.345 Å. The $C_{20}H_{21}^+$ B3LYP/6-31G* proton affinity (PA) is 185.3 kcal/mol (Table 4). Protonated ethane also has a proton-bridged C−C bond but with a lower PA (142.5 kcal/mol).[25] The larger PA of **1** is a size effect because the charge is better dispersed than in ethane. For comparison, we have also calculated a face-protonated exohedral C_{5v} $C_{20}H_{21}^+$ form, with the proton over the midpoint of a five-membered ring (Figure 1b). However, this is not a minimum ($N_{imag} = 2$) and is 31.6 kcal/mol higher in energy than the C_{2v} $C_{20}H_{21}^+$ geometry.

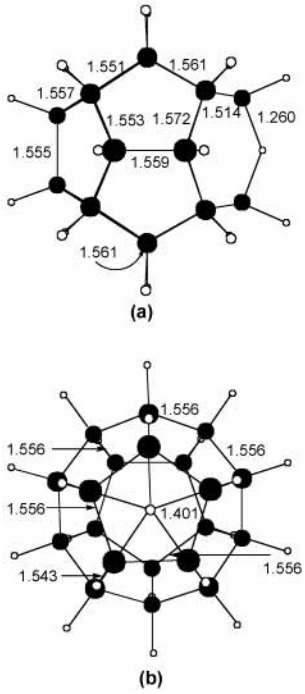

Figure 1. (a) C_{2v} bond- and (b) C_{5v} face-protonated dodecahedranes.

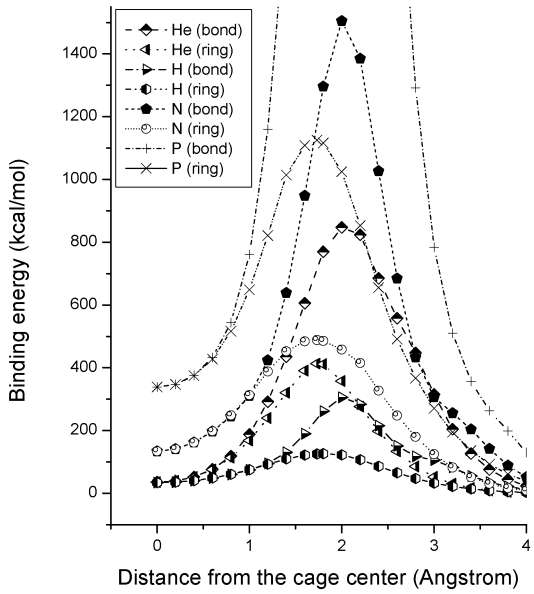

Figure 2. Energy of $X@C_{20}H_{20}$ (X= He, H, N, P) versus X distance from the cage center along bond-crossing and ring-crossing routes. For X = P, the maximum is reached at 4330 kcal/mol (not shown).

$X@C_{20}H_{20}$ (X = H, N, P). The cage-centered H, N, and P endohedral complexes are local minima. The hydrogen atom

TABLE 3: Selected B3LYP/6-31G* Optimized $XC_{20}H_{20}$ (Figure 3) Bond Angles (α−γ; degrees) and Bond Lengths (a−e; Å)

$XC_{20}H_{20}$	sym	α	β	γ	*a*	*b*	*c*	*d*	*e*	C_X	S_X	S_C
$^1H^+C_{20}H_{20}$	C_{2v}	116.1	107.4	136.9	1.261	1.514	1.572			0.26		
$^2HC_{20}H_{20}$	C_{2v}	116.9	103.5	144.8	1.325	1.526	1.577			0.26	−0.09	0.55
$^2HC_{20}H_{20}$	C_s	119.1	121.3	114.5	1.090	1.545	1.572	1.590	1.491	0.44	0.00	0.98
$^4NC_{20}H_{20}$	C_{2v}	115.9	110.0	123.2	1.381	1.582	1.547			0.03	1.31	0.0
$^2NC_{20}H_{20}$	C_{2v}	116.1	114.1	111.1	1.44x	1.567	1.557			−0.28	0.88	−0.06
$^4PC_{20}H_{20}$	C_{2v}	123.3	100.6	114.8	2.035	1.543	1.613			0.52	1.97	0.41
$^4PC_{20}H_{20}$	C_s	118.1	125.1	122.5	1.871	1.561	1.575	1.587	1.485	0.33	1.95	1.00
$^2PC_{20}H_{20}$	C_{2v}	119.2	114.5	93.2	1.862	1.557	1.566			0.64	0.98	−0.04
$^4C^-C_{20}H_{20}$	C_{2v}	116.8	111.1	117.6	1.468	1.570	1.559			0.16	1.80	−0.08
$^2C^-C_{20}H_{20}$	C_{2v}	116.3	116.0	104.2	1.525	1.575	1.561			−0.40	0.90	−0.05
$^4Si^-C_{20}H_{20}$	C_{2v}	120.9	110.9	98.7	1.902	1.556	1.566			0.78	1.735	0.07
$^2Si^-C_{20}H_{20}$	C_{2v}	119.6	115.8	87.6	1.987	1.552	1.571			0.20	1.00	−0.03
$^4O^+C_{20}H_{20}$	C_{2v}	122.5	99.7	126.2	1.747	1.534	1.590			0.09	1.37	0.54
$^4O^+C_{20}H_{20}$	C_s	117.5	122.7	120.5	1.269	1.670	1.545	1.601	1.485	−0.112	1.04	0.99
$^2O^+C_{20}H_{20}$	C_{2v}	114.5	113.5	116.9	1.390	1.558	1.549			−0.33	0.36	0.04
$^4S^+C_{20}H_{20}$	C_{2v}	124.5	98.7	116.8	2.021	1.542	1.609			0.71	1.61	0.47
$^4S^+C_{20}H_{20}$	C_s	117.1	125.0	120.3	1.748	1.592	1.565	1.592	1.483	0.68	1.53	1.01
$^2S^+C_{20}H_{20}$	C_{2v}	119.1	113.1	97.7	1.791	1.570	1.560			0.84	0.76	−0.01

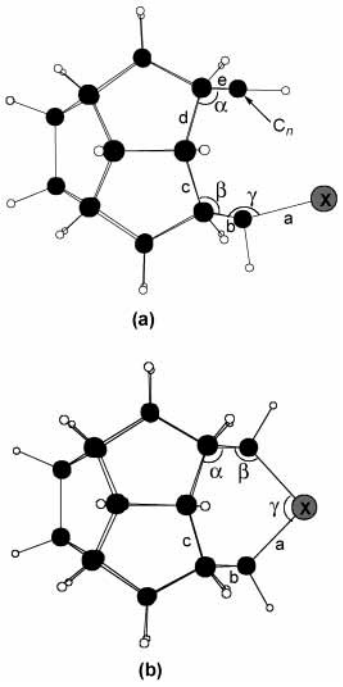

Figure 3. General structure of (a) C_s- and (b) C_{2v}-symmetric exohedral complexes. Optimized bond lengths and angles are summarized in Table 3.

TABLE 4: B3LYP/6-31G* Optimized X@C20H20 Absolute Energies (au), Zero-Point Energies (ZPE; kcal/mol, unscaled), Lowest Vibrational Frequencies (ω_1; cm^{-1}) (or Imaginary Frequencies), Exohedral Binding Energies (E_{bind}; kcal/mol), and Exohedral Endohedral Isomerization Energies (E_{isom}; kcal/mol) for Exohedral Isomers

		energy	ZPE	ω_1	E_{bind}	E_{isom}
$^1H^+C_{20}H_{20}$	C_{2v}	−774.48924	231.29	377.6	185.3	
$^2HC_{20}H_{20}$	C_{2v}	−774.68622	227.94	−1476.3i (1)[a]	1.7	
$^2HC_{20}H_{20}$	C_s	−774.70592	230.69	240.6	−7.9	44.2
$^4NC_{20}H_{20}$	C_{2v}	−828.65739	221.72	344.7	66.6	
$^2NC_{20}H_{20}$	C_{2v}	−828.86928	228.80	250.3	−125.7	191.7
$^4PC_{20}H_{20}$	C_{2v}	−1115.28700	222.65	−729.7i(1)[a]	95.1	
$^4PC_{20}H_{20}$	C_s	−1115.37763	223.90	102.8	39.4	
$^2PC_{20}H_{20}$	C_{2v}	−1115.49135	226.75	192.4	−69.3	329.4
$^4C^-C_{20}H_{20}$	C_{2v}	−812.07143	222.21	862.8	−29.8	
$^2C^-C_{20}H_{20}$	C_{2v}	−812.14252	225.41	225.2	−118.5	187.2
$^4Si^-C_{20}H_{20}$	C_{2v}	−1063.48822	219.79	233.2	59.1	
$^2Si^-C_{20}H_{20}$	C_{2v}	−1063.62338	224.29	179.6	−50.2	326.5
$^4O^+C_{20}H_{20}$	C_{2v}	−848.84593	218.58	−1339.9(3)[a]	−78.6	
$^4O^+C_{20}H_{20}$	C_s	−848.95550	221.75	162.6	−144.2	
$^2O^+C_{20}H_{20}$	C_{2v}	−849.10212	226.82	215.4	−321.6	210.3
$^4S^+C_{20}H_{20}$	C_{2v}	−1171.88432	221.87	−811.1i(1)[a]	9.3	
$^4S^+C_{20}H_{20}$	C_s	−1171.95646	222.03	104.8	−35.8	
$^2S^+C_{20}H_{20}$	C_{2v}	−1172.09019	226.75	178.8	−167.5	297.3

[a] Transition state or higher saddle point, with the number of the imaginary frequencies are given in parentheses.

and helium have nearly the same inclusion energy (36.3 vs 38.0 kcal/mol), but the inclusion energies of N and P are much higher (125.3 and 300.3 kcal/mol, respectively). Thus, H, N, and P encapsulations are unfavorable energetically. The inclusion energies of H and He at the B3LYP/6-31G* + ZPE level are in good agreement with our previously reported B3LYP/6-311+G(d,p) + ZPE results.[15c]

To determine whether the cage-centered configurations are the global minima for the endohedral complexes, the potential energy surfaces (PES) have been studied by moving the guest atoms in the fixed-cage host (Figure 2). Two extreme conditions for the guest to penetrate the cage have been investigated: one is ring crossing, which is simulated by displacing the guest atoms along the 5-fold axis from the cage center though a pentagonal surface to the exterior of the molecule, and the other is bond crossing, which is simulated by displacing the guest from the cage center to the C−C bond center and further to the exterior. The PES shown in Figure 2 indicates that the configurations with the guest at the cage center have the lowest energy and that the energy increases monotonically along both ring-crossing and bond-crossing routes to the exterior. The PES for off-center displacements confirms that H/N/P atoms are located at the cage center.

The net charges and spin densities of $X@C_{20}H_{20}$ (X = H, N, P) are listed in Table 2. There is negligible electron transfer between hydrogen and the cage framework. With a spin density of 0.91e, hydrogen nearly maintains its unencapsulated atomic electron configuration. N and P are much larger than H, and their host−guest interactions are greater. The encapsulated nitrogen atom accepts 0.05e from the cage and has a spin density of 2.57e, thus it still can be considered to preserve its atomic quartet ground-state approximately. Phosphorus, however, donates 1.07e to the cage and has a spin density of 1.73, indicating heavy orbital mixing with the framework of **1**.

As expected, all of the exohedral isomers are much more stable than their endohedral analogues. (See Table 4.) The most stable $HC_{20}H_{20}$ structure has a −7.9 kcal/mol hydrogen binding energy and is C_s-symmetric, with a CH_2 group and a ruptured C−C bond (Figure 3a). The increase in $C_{20}H_{20}$ strain energy when the cage is broken is smaller than the bond energy of the new C−H bond, hence a ruptured cage structure is preferred.

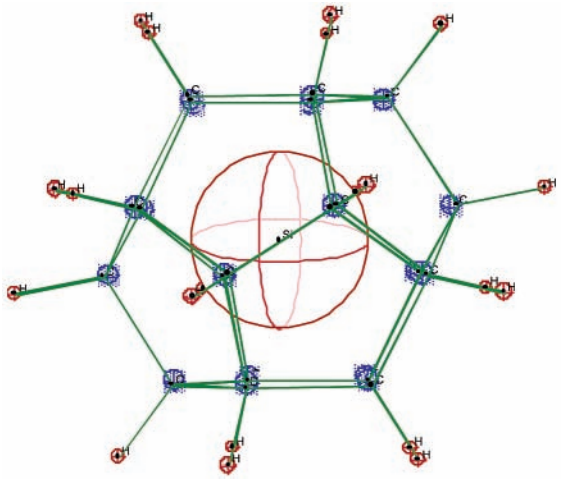

Figure 4. HOMO of B3LYP/6-31G*-optimized and I_h-symmetric $^4Si^-@C_{20}H_{20}$. The $^4Si^-$ encapsulating cage (C−C = 1.597 Å) is more compact than $^4Si^+@C_{20}H_{20}$ (C−C = 1.614 Å) because of electron donation from the anion center into the C−C bonding HOMO as shown. This is opposite to the ionic radii of their respective endohedral species (i.e., $^4Si^- > {}^4Si^+$).

The C_{2v} structure (Figure 3b) with hydrogen symmetrically inserted into a C−C bond is a transition state and only slightly higher in energy (by 1.7 kcal/mol) than its infinitely separated components. This very low dissociation energy is also due to the smaller strain energy in $C_{20}H_{20}$ than in the ruptured cage.

Both doublet and quartet states of C_{2v} $NC_{20}H_{20}$ are local minima (Figure 3b). The exohedral doublet complex is 125.7 kcal/mol more stable than the infinitely separated components, and the exohedral quartet is unstable by 66.6 kcal/mol toward dissociation into $C_{20}H_{20}$ and ^4N. The 192.3 kcal/mol energy difference between the doublet and quartet exohedral binding energies is much larger than the doublet−quartet separation of atomic nitrogen (66.2 kcal/mol). Similarly, exohedral doublet $PC_{20}H_{20}$ has a C_{2v} minimum with phosphorus binding to a C−C bond (Figure 3b) and is energetically more favorable by 69.3 kcal/mol than its independent components. In contrast, the C_{2v} structure is a transition state toward dissociation for exohedral quartet $^4PC_{20}H_{20}$; the C_s-symmetric structure with a CHP group and a ruptured C−C bond (Figure 3a) is a local minimum but is much higher in energy than the doublet state. E_{isom} is the smallest for encapsulated H (44.2 kcal/mol), whereas the endo → exo isomerization energies for N and P are very exothermic, approximately 192 and 329 kcal/mol, respectively.

$X@C_{20}H_{20}$ ($X = C^-, Si^-, O^+, S^+$). Quartet N and P are minima in the cage center because of their half-filled valence shells and spherically distributed wave functions. What is the nature of their isoelectronic charged analogues C^-, Si^-, O^+, and S^+ with half-filled shells? Except for $O^+@C_{20}H_{20}$, which is a third-order saddle point, all of the other ionic species are local I_h minima but are highly unstable (by 116−305 kcal/mol) toward dissociation. The exohedral low-spin complexes have significant binding energies ranging from −50 to −322 kcal/mol. The relative isomerization energies favoring exohedral over endohedral complexes are very high, in the 187−327 kcal/mol range (Table 4).

Both low- and high-spin C_{2v} $XC_{20}H_{20}$ ($X = C^-, Si^-$) species are minima. The high-spin complexes, $O^+C_{20}H_{20}$ and $S^+C_{20}H_{20}$, favor C_s structures, and their C_{2v} forms are transition states with very weak C−X bonds. In high-spin I_h endohedral complexes, C^-, O^+, and S^+ have spin densities of 2.12e, 2.23e, and 2.06e, respectively, and their quartet ground states are preserved approximately. However, with a spin density of 0.93e, Si^- loses its atomic ground-state character at the cage center.

The endohedral-complex cage bond lengths in the optimized geometries reveal subtle trends. Previously,[15c] we showed that cage C−C bonds shortened (<0.01 Å) and C−H bonds lengthened (≤0.02 Å) in response to electron donation into the C−C bonding and C−H antibonding HOMOs of endohedral complexes. The same trend is apparent in the quartet state $X@C_{20}H_{20}$ bond lengths, as shown in Table 1. The trend in atomic radii is $Si^- > P > S^+$, yet the C−C bond lengths decrease over the series $^4S^+@C_{20}H_{20}$ (1.614 Å) > $^4P@C_{20}H_{20}$ (1.608 Å) > $^4Si^-@C_{20}H_{20}$ (1.597 Å). That is, the cage shrinks when encapsulating large species, whereas the C−H bonds lengthen slightly. Similarly, the radius of C^- is larger than that of N, but the cage C−C bonds lengthen and C−H bonds shorten when going from $^4C^-@C_{20}H_{20}$ to $^4N@C_{20}H_{20}$. These bond-length alternations are explained qualitatively by the $X@C_{20}H_{20}$ HOMO, which resembles the C−C bonding and C−H antibonding $C_{20}H_{20}$ LUMOs in compact cages such as $^4Si^-@C_{20}H_{20}$ (Figure 4).

Conclusions

In summary, B3LYP density functional studies have located endohedral dodecahedrane minima and predict their stability toward dissociation. A proton (H^+) is not endohedrally encapsulated but prefers attachment to the external dodecahedrane surface. The $C_{20}H_{21}^+$ minimum is an exohedral complex whose proton bridges two carbons with a 2.35 Å C−C distance. H, N, P, and their isoelectronic species (C^-, Si^-, S^+) have local minima at the cage center, but O^+ does not. H has an endothermic inclusion energy (36.3 kcal/mol) similar to that of helium (38.0 kcal/mol), whereas the larger species (N, P, C^-, Si^-, O^+, and S^+) have much higher inclusion energies (ca. 125−305 kcal/mol). The exohedral complexes are favorable for all species. $C_{20}H_{21}$ prefers a structure with a CH_2 group and a ruptured C−C bond. N, P, and their isoelectronic analogues favor doublet exohedral complexes with symmetrical skeletally bound atoms. A low-energy ion beam colliding with $C_{20}H_{20}$ should result in exohedral complexes for all of these species, whereas a high-energy beam might result in the endohedral species for endohedral complexes between dodecahedrane and H, N, and P and their isoelectronic species (C^-, Si^-, S^+). Encapsulated H, N, C^-, O^+, and S^+ preserve their atomic ground states and thus are promising electron spin quantum-computing nanodevices, whereas P and Si^- interact with the cage strongly and their electronic states mix.

Acknowledgment. We thank the Deutsche Forschungsgemeinschaft (DFG/Erlangen), the University of Georgia, the U.S. National Science Foundation (grant CHE-0209857), and the Fonds der Chemischen Industrie for financial support and Professor Eluvathingal D. Jemmis (University of Hyderabad, India) for fruitful discussions. Z.C. thanks the Alexander von Humboldt Foundation for a fellowship.

Note Added in Proof

Following the acceptance of this paper for publication, a paper (Mascal, M. *J. Org. Chem.* **2002**, *67*, 8644) appeared reporting the activation barriers and reaction coordinate energy profiles for the penetration of H^+, He, Li^+, Be^+, Be^{2+}, and Mg^{2+} into dodecahedrane.

References and Notes

(1) (a) Paquette, L. A. *Chem. Rev.* **1989**, *89*, 1051. (b) Eaton, P. E. *Tetrahedron* **1979**, *35*, 2189. (c) Eaton, P. E. *Top. Curr. Chem.* **1979**, *79*, 41.

(2) (a) Engler, E. M.; Andose, J. D.; Schleyer, P. v. R. *J. Am. Chem. Soc.* **1973**, *95*, 8005. (b) Allinger, N. L. *J. Am. Chem.* Soc. **1977**, *99*, 8127. (c) Allinger, N. L.; Geise, H. J.; Pyckhout, W.; Paquette, L. A.; Gallucci, J. C. *J. Am. Chem. Soc.* **1989**, *111*, 1106.

(3) (a) Schulman, J. M.; Disch, R. L. *J. Am. Chem. Soc.* **1978**, *100*, 5677. (b) Dixon, D. A.; Deerfield, D.; Graham, G. D. *Chem. Phys. Lett.* **1981**, *78*, 161. (c) Schulman, J. M.; Disch, R. L. *J. Am. Chem. Soc.* **1984**, *106*, 1202. (d) Disch, R. L.; Schulman, J. M.; Sabio, M. L. *J. Am. Chem. Soc*. **1985**, *107*, 1904. (e) Scamehorn, C. A.; Hermiller, S. M.; Pitzer, R. M. *J. Chem. Phys*. **1986**, *84*, 833. (f) Disch, R. L.; Schulman, J. M. *J. Phys. Chem*. **1996**, *109*, 3504.

(4) Ermer, O. *Angew. Chem., Int. Ed. Engl.* **1977**, *16*, 411.

(5) Hudson, B. S.; Braden, D. A.; Parker, S. F.; Prinzbach, H. *Angew. Chem., Int. Ed.* **2000**, *39*, 514.

(6) Wahl, F.; Wörth, J.; Prinzbach, H. *Angew. Chem., Int. Ed. Engl*. **1993**, *32*, 1722.

(7) Schulman, J. M.; Venanzi, T.; Disch, R. L. *J. Am. Chem. Soc.* **1975**, *97*, 5335.

(8) Paquette, L. A.; Ternansky, R. J.; Balogh, D. W.; Kentgen, G. *J. Am. Chem. Soc*. **1983**, *105*, 5446.

(9) (a) Fessner, W. D.; Murty, B. A. R. C.; Wörth, J.; Hunkler, D.; Fritz, H.; Prinzbach, H.; Roth, W. D.; Schleyer, P. v. R.; McEwen, A. B.; Maier, W. F. *Angew. Chem., Int Ed. Engl.* **1987**, *26*, 452. (b) Bertau, M.; Wahl, F.; Weiler, A.; Scheumann, K.; Worth, J.; Keller, M.; Prinzbach, H. *Tetrahedron* **1997**, *53*, 10029. (c) Bertau, M.; Leonhardt, J.; Weiler, A.; Weber, K.; Prinzbach, H. *Chem.—Eur. J.* **1996**, *2*, 570.

(10) Beckhaus, H.-D.; Rüchardt, C.; Lagerwall; Paquette, L. A.; Wahl, F.; Prinzbach, H. *J. Am. Chem. Soc*. **1994**, *116*, 11775.

(11) Broadus, K. M.; Kass, S. R.; Osswald, T.; Prinzbach, H. *J. Am. Chem. Soc*. **2000**, *122*, 10964.

(12) (a) Paquette, L. A. In *Cage Hydrocarbons*; Olah, G. A., Ed.; Wiley & Sons: New York, 1990; pp 313−352. (b) Fessner, W. D.; Prinzbach, H. In *Cage Hydrocarbons*; Olah, G. A., Ed.; Wiley & Sons: New York, 1990; pp 353−405. (c) Prinzbach, H.; Weber, K. *Angew. Chem., Int. Ed. Engl.* **1994**, *33*, 2239.

(13) Prinzbach, H.; Weller, A.; Landenberger, P.; Wahl, F.; Worth, J.; Scott, L. T.; Gelmont, M.; Olevano, D.; v. Issendorff, B. *Nature (London)* **2000**, *407*, 60.

(14) (a) Disch, R. L.; Schulman, J. M. *J. Am. Chem. Soc.* **1981**, *103*, 3297. (b) Jiménez-Vázquez, H. A.; Tamariz, J.; Cross, R. J. *J. Phys. Chem. A* **2001**, *105*, 1315.

(15) (a) Chen, Z.; Jiao, H.; Bühl, M.; Hirsch, A.; Thiel, W. *Theor. Chem. Acc.* **2001**, *106*, 352. (b) Jimenez-Vazquez, H. A.; Tamariz, J.; Cross, R. J. *J. Phys. Chem. A* **2001**, *105*, 1315. (c) Moran, D.; Stahl, F.; Jemmis, E. D.; Schaefer, H. F., III; Schleyer, P. v. R. *J. Phys. Chem. A* **2002**, *106*, 5144.

(16) Cross, R. J.; Saunders, M.; Prinzbach, H. *Org. Lett*. **1999**, *1*, 1479.

(17) (a) Saunders, M.; Jiménez-Vázquez, H. A.; Cross, R. J.; Poreda, R. J. *Science (Washington, D.C.)* **1993**, *259*, 1428. (b) Saunders, M.; Cross, R. J.; Jiménez-Vázquez, H. A.; Shimshi, R.; Khong, A. *Science (Washington, D.C.)* **1996**, *271*, 1693.

(18) (a) Harneit, W.; Waiblinger, M.; Meyer, C.; Lips, K.; Weidinger, A. *Proc. Electrochem. Soc.* **2001**, *11*, 358. (b) Meyer, C.; Harneit, W.; Waiblinger, M.; Lips, K.; Weidinger, A. *AIP Conference Proceedings* **2001**, *591*, 101. (c) Harneit, W.; Waiblinger, M.; Lips, K.; Makarov, S.; Weidinger, A. *AIP Conf. Proc.* **2000**, *544*, 207. (d) Park, S.; Srivastava, D.; Cho, K. *J. Nanosci. Nanotech*. **2001**, *1*, 1. (e) Harneit, W. *Phys. Rev. A* **2002**, *65*, 032322.

(19) Sahoo, R. R.; Patnaik, A. *Chem. Phys. Lett.* **2001**, *349*, 201.

(20) (a) Almeida, M. T.; Pawlik, T.; Weidinger, A.; Höhne, M.; Alcala, R.; Spaeth, J. M. *Phys. Rev. Lett.* **1996**, *77*, 1075. (b) Knapp, C.; Dinse, K. P.; Pietzak, B.; Waiblinger, M.; Weidinger, A. *Chem. Phys. Lett*. **1997**, *272*, 433. (c) Pietzak, B.; Waiblinger, M.; Almeida, M. T.; Weidinger, A.; Höhne, M.; Dietel, E.; Hirsch, A. *Chem. Phys. Lett.* **1997**, *279*, 259.

(21) Knapp, C.; Weiden, N.; Kass, K.; Dinse, K. P.; Pietzak, B.; Waiblinger, M.; Weidinger, A. *Mol. Phys*. **1998**, 95, 999.

(22) Smith, R.; Beardmore, K.; Belbruno, *J. Chem. Phys*. **1999**, *111*, 9227.

(23) Frisch, M. J.; Trucks, G. W.; Schlegel, H. B.; Scuseria, G. E.; Robb, M. A.; Cheeseman, J. R.; Zakrzewski, V. G.; Montgomery, J. A., Jr.; Stratmann, R. E.; Burant, J. C.; Dapprich, S.; Millam, J. M.; Daniels, A. D.; Kudin, K. N.; Strain, M. C.; Farkas, O.; Tomasi, J.; Barone, V.; Cossi, M.; Cammi, R.; Mennucci, B.; Pomelli, C.; Adamo, C.; Clifford, S.; Ochterski, J.; Petersson, G. A.; Ayala, P. Y.; Cui, Q.; Morokuma, K.; Malick, D. K.; Rabuck, A. D.; Raghavachari, K.; Foresman, J. B.; Cioslowski, J.; Ortiz, J. V.; Stefanov, B. B.; Liu, G.; Liashenko, A.; Piskorz, P.; Komaromi, I.; Gomperts, R.; Martin, R. L.; Fox, D. J.; Keith, T.; Al-Laham, M. A.; Peng, C. Y.; Nanayakkara, A.; Gonzalez, C.; Challacombe, M.; Gill, P. M. W.; Johnson, B. G.; Chen, W.; Wong, M. W.; Andres, J. L.; Head-Gordon, M.; Replogle, E. S.; Pople, J. A. *Gaussian 98*, revision A.5; Gaussian, Inc.: Pittsburgh, PA, 1998.

(24) Glendening, E. D.; Badenhoop, J. K.; Reed, A. E.; Carpenter, J. E.; Weinhold, F. *NBO*, version 4.0; University of Wisconsin: Madison, WI, 1996.

(25) (a) Carneiro, J. W. d. M.; Schleyer, P. v. R.; Saunders: M.; Remington, R.; Schaefer, H. F., III.; Rauk, A.; Sorensen, T. S. *J. Am. Chem. Soc*. **1994**, *116*, 3483. (b) Bohme, D. K.; Mackay, G. I. *J. Am. Chem. Soc*. **1981**, *103*, 2173.